"Rheological characterization platforms for the extrudability and safety analysis of energetic materials "

Proceedings of AICHE Annual Meeting Austin, Texas
Processing and Safety of Energetics Materials Session
November 11, 2004

Dilhan M. Kalyon
dkalyon@stevens.edu

Stevens Institute of Technology, Castle Point
Hoboken, NJ 07030

Synopsis

Energetic materials including gun propellants, solid rocket fuels, and pyrotechniques involve polymeric binders filled with energetic particles at concentrations that generally approach the maximum packing fraction of the solid phase. The high volume fraction of solids, which could be as high as over 80 percent by volume, gives rise to viscoplasticity coupled with wall slip. Thus, the characterization of the rheological behavior of the energetic formulations necessitates methods for the determination of the wall slip velocity values and the true wall shear rate and some way of determining the yield stress of the suspension. Here such methodologies for the characterization of the shear viscosity material function employing various basic viscometric flows, i.e., capillary, rectangular slit, steady torsional, cone-and-plate and squeeze flows are outlined. The energetic suspension is assumed to be incompressible and flow under fully-developed conditions subject to apparent slip. The apparent slip layer is assumed to consist solely of the binder of the energetic formulation and its thickness is assumed to be independent of the flow rate. Both the drag induced (plane Couette) and pressure induced (capillary and slit) flows generate the same dependencies of the slip velocity on the shear stress for Newtonian and non-Newtonian binders under isothermal and creeping flow conditions. Navier´s slip coefficient, which relates the wall slip velocity to the shear stress, is determined to be similar for all three flows and is a function of the apparent slip layer thickness and the shear viscosity of the binder. The assumed apparent slip mechanism provides slip velocity values that are consistent with the traditional Mooney method and furthermore allows the determination of the true shear rate of the energetic suspension at the wall. The yield stress value of the energetic suspension is determined as a byproduct of the wall slip analysis. The characterization of the rheological behavior of the energetic suspension generally requires multiple methods overlapping in their shear rate ranges to be applied. The understanding of the rheological behavior of the energetic material is a must for its processing under safe conditions.

Introduction

Energetic suspensions including solid rocket fuels, gun propellants and pyrotechniques are concentrated suspensions of particulate solids in polymeric binders. The rheological characterization of such concentrated suspensions is complicated by their viscoplasticity [Bingham (1922)], their ubiquitous slip at the walls of the rheometers [Reiner (1960)] and various types of migration [Leighton and Acrivos (1987)] and structure development effects [Metzner (1985)]. Capillary, slit and steady torsional flows are most frequently employed for the characterization of the wall slip behavior of suspensions [Yilmazer and Kalyon (1989); Barnes (1995)]. Among these three flows, historically the capillary flow has been the most commonly applied since the theoretical basis for the wall slip analysis in capillary flow has been established since 1931 [Mooney (1931)]. The methodology of "Mooney method", involves changing the surface to volume ratio of the capillary die, i.e., by using capillary dies with differing diameters at constant length over diameter ratio. The wall slip versus the wall shear stress behavior of a number of concentrated suspensions has been characterized using the Mooney analysis method [Yilmazer and Kalyon (1989 and 1991); Kalyon et al. (1993); Aral and Kalyon (1994); Michienzi et al. (1997); Suwardie et al. (1998); Kalyon et al. (1999); Prickett et al. (2003)].

The adoption of the Mooney method to steady torsional flow has been carried out by Yoshimura and Prud'homme by changing the surface to volume ratio of the rheometer, i.e., the gap between the disks [Yoshimura and Prud'homme (1988)]. Kalyon et al. (1993) have investigated the applicability of this correction method to steady torsional flow by comparing the wall slip velocity values inferred from the gap dependence of the apparent viscosity, obtained upon the use of Mooney analysis, with the wall slip velocity versus wall shear stress data obtained independently by using a straight-line marker technique in steady torsional flow.

A combination of drag-induced (steady torsional flow) and pressure-induced (capillary) flows was used to characterize the wall slip velocity values over a broad range of shear stresses [Yilmazer and Kalyon (1989) and Kalyon et al. (1993)]. These studies have shown that the wall slip behavior remains the same for both flows, suggesting that the mechanisms of wall slip are likely to be the same for both the drag induced and pressure induced rheometers. Various methodologies were also developed to characterize the "true" (slip corrected) shear viscosity of the suspension upon the determination of the wall slip velocity versus wall shear stress behavior [Yilmazer and Kalyon (1991); Aral and Kalyon (1994); Kalyon et. al. (1993); Kalyon (2003)]. The determination of the wall slip velocities by systematically changing the surface to volume ratio of the rectangular slit die rheometer has also been carried out [Kalyon et al. (1997)] in conjunction with an in-line slit die with a continuously adjustable gap [Kalyon and Gokturk (1994)]. The applicability of the inverse problem solution techniques to parameter estimation of viscoplastic fluids, subject to wall slip, was also investigated [Yeow et al. (2003); Tang and Kalyon (2004)]

The migrations of particle and binder during viscometric flows of concentrated suspensions are affected by wall slip. Acrivos and co-workers have determined the wall slip velocity values of a concentrated suspension from shear-induced particle migration effects occurring in Couette flow [Jana et al. (1995)]. Allende and Kalyon (2000) have demonstrated the effect of wall slip on the migration of particles in the transverse to flow direction in Poiseuille flow. The wall slip of the suspension also affects the filtration-based migration of the binder.

The migration of the particles represents a quality issue, since it can be assumed that the particles with the smaller diameters, i.e., the greater surface to volume ratio, would give rise to significant differences in burn rates. Thus, the effect of significant migration of particles in the transverse to flow direction would be to alter the burn rate distributions across the grain. On the other hand, the migration of the binder in the axial flow direction (in the direction of the pressure gradient) represents a serious safety issue.

As shown by Yilmazer et al. (1989a) and Yaras et al. (1994) the migration of the binder depletes the concentration of the binder in the processor. In extreme cases it is shown that the suspension becomes unprocessable. The migration of the binder phase is believed to be the cause of some of the incidents. For example, in one case involving a single screw extrusion process the binder wax was observed to exude out of the die of the extruder first followed by an explosion. As shown by Yilmazer et al. (1989a), this incident fits the grinding mechanism that ensues in the extruder when the suspension in the mixing volume loses some of its binder, becomes solid-like and the continuation of the rotation of the screws leads to the grinding of the particles of the suspension.

Since the concentration of solids approaches the maximum packing fraction in most energetic suspensions, the rheological behavior and the processability of energetic suspensions are very sensitive to the amount and distribution of air entrained during processing [Kalyon et al. 1991 a]. Air entrainment is related to the geometry and operating conditions employed during processing, especially on the degree of fill distribution in the continuous processor [Kalyon et al. 1991 b]. Thus, the shear viscosity and wall slip behavior of a given suspension can be altered on the basis of tailoring its air content in the confines of the processor [Kalyon et al. (1991)].

Thus, the experimental methods of obtaining the wall slip behavior of energetic suspensions as a function of the wall shear stress are available. However, currently there is no a priori method of estimating and predicting their wall slip behavior. Furthermore, the mechanisms involved in the development of the slip velocity behavior are not clear. Finally, there is no clear-cut methodology for the determination of the yield stress value of an energetic suspension. Here the development of the apparent slip mechanism upon the formation of a thin slip layer at the wall, consisting solely of the binder, is used as the basis for solving the velocity distributions of viscoplastic fluids in plane Couette, capillary and rectangular slit flows and the determination of the corresponding wall shear rate. These distributions allow the determination of the relationships between the wall slip velocity and the shear stress on one hand and the development of the flow curves for these rheometers on the other hand. The consistency of this mechanism with the traditional Mooney method, for the determination of the slip velocities, is also investigated. Finally, correlations of the wall slip behavior with various properties of the concentrated suspensions are sought.

Apparent slip mechanism

During the flow of a suspension of rigid particles the particles cannot physically occupy the space adjacent to a wall as efficiently as they can away from the wall. This leads to the formation of generally relatively thin but always present layer of fluid adjacent to the wall, i.e., the “apparent slip layer” or the “Vand layer”. Green detected this layer as early as 1920 in the flow of paint suspensions under a microscope [Green (1920]. According to Bingham: “slip comes from a lack of adhesion between the material and the shearing surface. The result is that there is a layer of liquid between the shearing surface and the main body of the suspension and flow takes place in this layer according to the laws of viscous rather than plastic flow" [Bingham (1922)]. If the dispersion medium consists of a structured fluid, its shear viscosity will vary with structuring parameters. For example, it has been shown that in the case of oleic acid forming the apparent slip layer the orientation of the oleic acid molecules, parallel to the wall, reduces "friction", i.e., oleic acid acts as a lubricant [Reiner (1960)]. On the other hand, when the molecules of oleic acid are oriented normal to the wall "friction increases", i.e., oleic acid at the wall acts as a "roughening layer" [Reiner (1960)].

The development of this apparent wall slip layer has important ramifications in processing and manufacturing, process control, rheological characterization and properties of energetic suspensions. The formation of a slip layer during processing in dies, extruders and in various molding, and shaping machinery, changes the processability characteristics of the energetic suspension. For example, in single and twin screw extrusion wall slip reduces the pressurization rate of the extruder and its distributive and dispersive mixing capabilities [Kalyon (1993, 1995)]. In die flows wall slip reduces the pressure drop, the viscous energy dissipation and particle migration effects [Allende and Kalyon (2000)].

The formation of the slip layer thickness does complicate efforts to characterize in-line the physical and chemical characteristics of energetic suspensions during manufacture. For example, various sensors that are based on infrared signals need to penetrate beyond the thickness of the slip layer to generate data, which are representative of the bulk of the suspension [Kalyon (1993, 1995)]. Furthermore, the slip layer becomes a "skin" upon solidification of the suspension upon processing, and alters the burn-rate, surface smoothness and mechanical properties of the extrudates of the energetic suspension. Thus, the development of the slip layer during deformation and flow of energetic suspensions is an important structuring effect with important ramifications for energetics manufacture.

Here it is assumed that the apparent slip layer thickness, δ, of an energetic suspension is free of particles and consists solely of the binder of the energetic suspension. This mechanism is depicted in an exaggerated manner in Figures 1 and 2, which show the apparent slip layers formed next to the walls in plane Couette flow and capillary/rectangular slit flows, respectively. For concentrated suspensions the shear viscosity of the binder of the suspension will be significantly smaller than the shear viscosity of the bulk of the suspension away from the wall, giving rise to a step change in the slope of the velocity distribution. Since the thickness of the slip layer, δ, is significantly smaller than the channel gap, the formation of the slip layer gives the appearance of wall slip; hence the "apparent slip" at the wall.

Let us probe the validity of this mechanism by directly analyzing the extrudates of an inert concentrated suspension, i.e., "a processing simulant". The suspension used for this demonstration has 76.3% by weight of KCl particles (61.9% by volume) incorporated into a binder consisting of a terpolymer based elastomer (Grade 4404 available from Zeon Chemicals, emulsion polymerized terpolymer of ethyl acrylate, butyl acrylate and hydroxyl cure site monomer) plasticized with a dioctyl adipate, DOA, plasticizer available from Eastman Chemical Company. The extrudates of this suspension could hold their shapes upon exit from a capillary die. The size distribution of the low aspect ratio KCl particles is bimodal with 31% of the KCl consisting of particles with a mean equivalent diameter of 72 microns and 69% of the KCl particles exhibiting a mean equivalent diameter of 176 microns.

The maximum packing fraction of the KCl particles is estimated as 0.68 following the method of Ouchiyama and Tanaka [Ouchiyama and Tanaka (1984) and Fiske et al. (1994)]. The harmonic mean diameter of the KCl particles is 121 microns. The suspension was extruded at 71 °C, from a capillary rheometer using various dies with differing diameters. The extrudates were collected, cryogenically fractured to expose their cross-sectional areas and their cross-sections were analyzed for the distributions of the binder and the particles using scanning electron microscopy and energy dispersive x-ray analysis.

Figure 3 shows a typical scanning electron micrograph (magnification ratio of 75X) of an extrudate section adjacent to the free surface of the extrudate. The diameter of the extrudate is 9 mm and thus only a small portion of the extrudate is captured in the micrograph. The thickness distribution of the particle-free binder layer found at the wall was determined at higher magnifications over the same section. Some of the identified particles of KCl are shown hatched, while the apparent slip layer is indicated as the black zone located adjacent to the free surface of the extrudate. The determination of the thickness distribution of the particle-free apparent slip layer revealed a mean value of 10.8 microns, a standard deviation of 6.3 microns and a range of 2 to 30 microns. Thus, the ratio of the mean thickness of the slip layer over the harmonic mean particle diameter of the rigid particles of the suspension is about 0.09.

This ratio is in the same approximate range of the earlier estimates of the ratios of the thickness of the apparent slip layer over the mean particle diameter determined for concentrated suspensions with Newtonian binders and non-colloidal particles. For example this ratio was determined as 0.06 by Yilmazer and Kalyon (1989) for a suspension filled with 60% by volume of ammonium sulfate particles and was determined to be 0.063 by Jana et al. (1995) for suspensions filled with poly(methyl methacrylate) particles in the range of 46 to 52% by volume. The ratios of the slip layer thickness over the particle diameter were determined to be 0.037 and 0.071 for glass beads and Al particles suspended in a Newtonian hydroxyl terminated polybutadiene binder, respectively [Soltani and Yilmazer (1998)].

Given this apparent slip mechanism what factors affect the development of the wall slip condition for an energetic suspension under steady state conditions? Is the apparent slip layer formation mechanism of the energetic material compatible with Mooney's method for the determination of the wall slip velocities? The assumptions for the analysis to follow are derived from those used by Reiner who assumed that the apparent slip layer of a suspension behaved as a Newtonian fluid [Reiner (1960)]:

a) The apparent slip layer consists solely of the binder of the suspension and itself adheres to the wall.
b) The thickness of the apparent slip layer is sufficiently small so that the separation of the binder from the bulk suspension to form the slip layers does not affect the shear viscosity of the suspension.
c) The thickness of the apparent slip layer is not affected by the radius of the flow channel nor the volumetric flow rate.
d) The binder fluid forming the apparent slip layer and the bulk suspension are incompressible and can be represented as generalized Newtonian fluids:

Velocity Distributions of Viscoplastic Suspensions with the Apparent Slip Mechanism for Drag and Pressure Induced Flows:

Here three viscometric flows involving both drag and pressure driven flows, i.e., the drag induced-plane Couette flow and pressure-driven flows through capillary and rectangular slit dies are analyzed. The velocity distributions, the flow rate versus the pressure drop behavior, the shear rate of the suspension at the interface with the apparent slip layer and the wall slip velocity versus the shear stress relationships were obtained. For the three fully developed simple shear flows considered here, there is one velocity component V_z which changes only in one transverse to flow direction i.e., $V_z(y)$ or $V_z(r)$ in Cartesian and cylindrical coordinate systems for the plane Couette and rectangular slit flows, and the capillary flows, respectively. In simple shear flow (with the transverse to flow direction y or r) the behavior of the suspension is represented by a Hershel-Bulkley type viscoplastic constitutive equation (- sign is used for negative shear stress):

$$\tau_{yz} = \pm\tau_0 - m\left|\frac{dV_z}{dy}\right|^{n-1}\left(\frac{dV_z}{dy}\right) \tag{1}$$

for the absolute value of the shear stress, $|\tau_{yz}| \geq \tau_{0,}$ i.e., the yield stress of the suspension, and the shear rate (dV_z/dy) = 0 for $|\tau_{yz}| < \tau_{0.}$ Here the shear rate sensitivity index, n, consistency index, m and the yield stress, τ_0**,** are the parameters of the Herschel-Bulkley equation of the suspension. The Ostwald-de Waele or "power law" behavior represents the behavior of the shear viscosity of the binder phase:

$$\tau_{yz} = -m_b\left|\frac{dV_z}{dy}\right|^{n_b-1}\left(\frac{dV_z}{dy}\right) \tag{2}$$

where m_b and n_b are the parameters of the Ostwald-de-Waele "power-law" equation. The analysis to follow, which uses a combination of the Hershel-Bulkley type viscoplastic bulk fluid and the power-law type binder to form the apparent slip layer, also provides as simplifications the cases of Bingham type viscoplastic bulk fluid (n=1), power-law type of bulk fluid (τ_0=0), and Newtonian bulk fluid (τ_0=0 and n=1) and the Newtonian binder fluid forming the apparent slip layer (n_b=1). They all simplify to the no-slip case upon setting the thickness of the apparent slip layer to zero, i.e., δ=0.

The slip velocity is the difference between the velocity of the fluid found at the interface, between the bulk suspension and the apparent slip layer, and the wall velocity. Thus, the slip velocity will be positive or negative for the plane Couette flow and will be positive for the pressure driven capillary and rectangular slit flows.

Plane Couette Flow (pure drag):

The isothermal plane Couette flow of an incompressible viscoplastic suspension under steady state and creeping flow conditions is considered first. The viscoplastic suspension is sandwiched in between two apparent slip layers consisting of the binder with thickness δ (Figure 1). The pressure gradient, (dP/dz) = 0. The fully developed velocity distribution within the apparent slip layer Zone I is given as:

$$V_z{}^{I} = \left(\frac{-\tau_{yz}}{m_b}\right)^{s_b} y \qquad \text{for } 0 \le y \le \delta \tag{3}$$

where $s_b = 1/n_b$ is the reciprocal power-law index from Equation (2). The velocity distribution of the deforming viscoplastic fluid, i.e., Zone II for $|\tau_{yz}| \ge \tau_0$ becomes:

$$V_z{}^{II} = \delta\left(\frac{-\tau_{yz}}{m_b}\right)^{s_b} + \left(\frac{-(\tau_{yz}+\tau_0)}{m}\right)^{s}(y-\delta) \qquad \text{for } \delta \le y \le (H-\delta) \tag{4}$$

where s=1/n and H is the distance of separation between the two infinitely wide and long plates. The velocity distribution in the apparent slip layer (Zone III), found adjacent to the upper wall moving with velocity $\overline{V}_w$, is:

$$V_z{}^{III} = \overline{V}_w + \left(\frac{-\tau_{yz}}{m_b}\right)^{s_b}(y-H) \qquad \text{for } (H-\delta) \le y \le H \tag{5}$$

The prevailing shear stress, τ_{yz}, is determined from:

$$\left(\frac{-(t_{yz}+t_0)}{m}\right)^{s}(1-2\,\delta^{*})+2\,\delta^{*}\left(\frac{-t_{yz}}{m_b}\right)^{s_b}=\frac{\overline{V}_w}{H} \qquad (6)$$

where δ^* is the normalized slip layer thickness, $\delta^* = \delta/H$.

The adoption of the Mooney's general methodology of differentiating the apparent shear rate with respect to inverse of the gap at constant shear stress to plane Couette flow provides the wall slip velocity, U_s from Equation (7):

$$\left.\frac{\partial\left(\overline{V}_w/H\right)}{\partial(1/H)}\right|_{t_{yz}}=2\,\delta\left(\frac{-t_{yz}}{m_b}\right)^{s_b}-2\delta\left(\frac{-(t_{yz}+t_0)}{m}\right)^{s}\cong 2\left.V_z^{I}\right|_{y=\delta}=2\left.U_s\right|_{y=\delta} \qquad (7)$$

The slip velocity, U_s, values are thus obtained as a function of the shear stress, τ_{yz} from the slopes of the apparent shear rate, $\overline{V}_w/H$, versus reciprocal gap separation (1/H) data. The y-intercept of $\overline{V}_w/H$ versus 1/H for $\delta << H$ is $\left(\frac{-(t_{yz}+t_0)}{m}\right)^{s}$, which in turn is equal to $\frac{dV_z^{II}}{dy}$, i.e., the true deformation rate of the suspension at the imposed shear stress, τ_{yz}.

Overall, the relationship between the apparent slip velocity, U_s and shear stress, τ_{yz} becomes:

$$U_s=\pm ß\left(-t_{yz}\right)^{s_b}=\pm\frac{\delta}{m_b^{\ s_b}}\left(-t_{yz}\right)^{s_b} \qquad (8)$$

Here ± is necessary to accommodate the apparent slip occurring adjacent to the moving surface and the stationary surface (Figure 1). The Navier´s slip coefficient, β, which relates the slip velocity, U_s to shear stress, τ_{yz}, is thus defined on the basis of the slip layer thickness, δ and parameters of the shear viscosity of the binder, i.e., m_b and $s_b = 1/n_b$.

$$\beta = \frac{\delta}{m_b^{s_b}} \tag{9}$$

Equation 9 suggests that the wall slip behavior of an energetic suspension can be predicted if the apparent slip layer thickness, δ, and the shear viscosity material function of the binder are known a priori.

This relationship of the Navier's slip coefficient with the shear stress has been verified for Newtonian binders by the slip velocity versus shear stress experiments [Aral and Kalyon (1994); Soltani and Yilmazer (1998)]. In those experiments the temperature was changed systematically to alter the shear viscosity of the Newtonian binder, μ_b, to demonstrate that the Navier's slip coefficient indeed obeys $U_s = \pm \frac{d}{\mu_b} t_w$.

Applications: Cone-and-plate flow

For the no-slip condition the shear rate within the gap is constant as Ω/θ_o, where Ω is the rotational speed of the cone. For the small cone angles, θ_o, used (generally $\theta_o < 2$) the gap H(r) between the cone and plate as a function of the radial distance, r, is θ_o r. The torque obtained at a given wall velocity, $\overline{V}_w = \Omega r$, can be converted to the corresponding shear stress [Bird et al. (2002)]. For the no-slip condition the shear stress is a constant between the cone and plate. The corresponding treatment for the apparent wall slip case by using Equation (7) furnishes the following shear stress, t_{yz}, for a Bingham type viscoplastic suspension (n=s=1) with a Newtonian binder ($s_b=n_b=1$):

$$t_{yz} = \frac{t_0(1-2\delta^*) + \frac{m\overline{V}_w}{H}}{1-2\delta^* + \frac{2m\delta^*}{m_b}} = \frac{t_0(1-2\delta^*) + m\frac{\Omega}{\theta_0}}{1-2\delta^* + \frac{2m\delta^*}{m_b}}$$

(10)

where $H = \theta_0 r$ and $\delta^* = \frac{\delta}{H} = \frac{\delta}{(\theta_0 r)}$. Thus, the shear stress, t_{yz}, becomes a constant in between the cone and plate under the conditions of either a negligible slip layer thickness, δ, over the gap ratio, δ*, or for δ* values which do not change significantly in the radial direction.

Steady torsional flow (parallel disks):

In steady torsional flow the dependence of the wall velocity, $\overline{V}_w$, on radial distance r, i.e., $\overline{V}_w = \Omega r$, generates a shear rate which is a function of the radial distance. The shear viscosity at the edge, i.e., r=R, $\eta(\dot{\gamma}_R)$, is:

$$\eta\left(\dot{\gamma}_R\right) = \frac{\dfrac{T}{2\pi R^3}}{\dot{\gamma}_R}\left[3 + \frac{d\ln T}{d\ln \dot{\gamma}_R}\right] \tag{11}$$

where T is the torque. For the no-slip condition the shear rate at the edge, $\dot{\gamma}_R$, is known, i.e., $\dot{\gamma}_R = \Omega$ R/H. However, for the apparent slip case there is no a priori way of determining the shear rate experienced by the suspension undergoing fully developed shear flow. The problem with applying a Mooney type analysis with this case is that the shear stress is non-linear with distance and is not known a priori [Brunn et al. (1996)]. Equation 11 can only be used if the shear rate of the suspension can be determined independently as a function of the torque applied. For example, the straight line marker technique together with cinematography (see Figure 4b) can provide the fully-developed values of the slip velocity, Us, and the true shear rate of the suspension at the edge, $\dot{\gamma}_R$, as part of the steady torsional flow experiment [Aral and Kalyon (1994)]. With such a technique (or any other which is able to measure the velocity distribution as part of the steady torsional flow experiment) the slope $\frac{d\ln T}{d\ln \dot{\gamma}_R}$ can be obtained from a series of torque, T versus $\dot{\gamma}_R$ data to provide the shear stress and the shear viscosity at the edge from Equation (11).

Capillary and Rectangular Slit Flows

In fully developed flows in capillary and rectangular slit dies the shear stress is linear with the distance in the transverse to flow direction, r, in capillary flow and y in rectangular slit flow, regardless of the constitutive equation of the fluid. The formation of a plug at shear stress values smaller than the yield stress, τ_0, is unavoidable for capillary and rectangular slit flows of viscoplastic fluids.

Capillary flow

Under fully developed and isothermal flow conditions the velocity profile in the apparent slip layer becomes:

$$V_z{}^{I} = \left[\frac{-dP}{dz}\frac{1}{2m_b}\right]^{s_b} \frac{R^{s_b+1}}{(s_b+1)}\left[1-\left(\frac{r}{R}\right)^{s_b+1}\right] \qquad (12)$$

where $\frac{-dP}{dz}$ is the pressure gradient for the fully developed flow and R is the radius of the capillary. The slip velocity $U_S = V_Z{}^{I}\Big|_{(R-\delta)}$ is:

$$U_s = \frac{\tau_w{}^{s_b}}{m_b{}^{s_b}}\frac{R}{(s_b+1)}\left[1-\left(1-\frac{\delta}{R}\right)^{s_b+1}\right] \qquad (13)$$

where $\tau_w = \frac{-dP}{dz}\frac{R}{2}$ is the wall shear stress. This provides the same functional relationship between the wall shear stress, τ_w, and slip velocity U_s as observed earlier for the plane Couette flow (Equation 10):

$$U_s = \beta\tau_w{}^{s_b} \qquad (14)$$

$$\text{where} \quad ß = \frac{R}{m_b^{s_b}(s_b+1)}\left[1-\left(1-\frac{d}{R}\right)^{s_b+1}\right] \tag{15}$$

Considering that the reciprocal power-law index $s_b = 1/n_b$ of the binder is positive –and assuming an integer value - the use of Binomial Theorem provides:

$$\left(1-\frac{d}{R}\right)^{s_b+1} \cong 1 - \frac{\delta}{R}(s_b+1) \tag{16}$$

generating a Navier's slip coefficient β of:

$$ß = \frac{d}{m_b^{s_b}} \text{ and } U_s = \frac{d}{m_b^{s_b}} t_w^{s_b} \tag{17}$$

Equation 17 was used by Jiang et al. (1986) and Yilmazer and Kalyon (1989) to determine the thickness of the apparent slip layer for a gel and a concentrated suspension, respectively. Thus, the parameters of the shear viscosity material function of the binder phase plus the slip layer thickness value are again shown to be sufficient to obtain an estimate of the wall slip behavior of a suspension.

Upon integration of the velocity distributions the volumetric flow rate, Q, becomes:

$$Q = \pi R^2 U_s \left[1 - \frac{\delta}{R} + \frac{(1 - s_b)}{3}\left(\frac{\delta}{R}\right)^2 + \frac{s_b(s_b+2)}{12}\left(\frac{\delta}{R}\right)^3 \right]$$

$$+ \left(\frac{\tau_w}{m}\right)^s \frac{\pi R^3}{(s+1)} \left[\left(1 - \frac{\delta}{R}\right)^2 \left(1 - \frac{\delta}{R} - \frac{\tau_0}{\tau_w}\right)^{s+1} \right.$$

$$\left. - \frac{2}{(s+3)}\left(1 - \frac{\delta}{R} - \frac{\tau_0}{\tau_w}\right)^{s+3} - \frac{2}{(s+2)}\left(1 - \frac{\delta}{R} - \frac{\tau_0}{\tau_w}\right)^{s+2} \frac{\tau_0}{\tau_w} \right]$$

(18)

The first term on the right of Equation (26) can be approximated as the volumetric flow rate due to slip, $Q_s = U_s \pi R^2$ since generally all terms involving δ/R are much smaller than 1.

The shear rate at r = R - δ i.e., $\left[- \frac{dV_z^{II}}{dr} \right]_{r=R-\delta}$ has a special significance.

$$- \frac{dV_z^{II}}{dr}\bigg|_{R-\delta} = \frac{(Q - Q_s)}{\pi R^3}\left[3 + \frac{d\ln(Q - Q_s)}{d\ln \tau_w} \right] \qquad (19)$$

and represents the deformation rate experienced by the suspension at the interface with the apparent slip layer (for R>>δ). It is the true shear rate of the suspension, which corresponds to the wall shear stress $\tau_{rz}|_{R-\delta} \approx \tau_w$. Equation 19 can also be directly obtained from the integration of the velocity distribution using Leibniz rule of integration without assuming a constitutive behavior for the bulk fluid [Kalyon (2003)]. Equation (19) becomes the conventional Rabinowitsch correction [Rabinowitsch (1929)] for the no slip condition, $Q_s = 0$. Rearranging Equation 19 as apparent shear rate, $\dot{\gamma}_a = \frac{4Q}{\pi R^3}$ versus reciprocal tube diameter (1/D) and taking the derivative of apparent shear rate with respect to reciprocal diameter of the tube (1/D) at constant wall shear stress for $\delta/R << 1$ generates the same result as provided by Mooney´s analysis for flow in a capillary [Mooney (1931)]:

$$\left.\frac{\partial\left(\frac{4Q}{\pi R^3}\right)}{\partial(1/D)}\right|_{\tau_w} = 8\,U_s\left(t_w\right) \qquad (20)$$

The transition from plug flow to a deforming suspension can be used to define the yield stress value of the suspension in capillary flow [Gevgilili (2003)]. At the transition $Q_s/Q = 1$ and $\tau_w = \tau_0$ for $\delta/R <<$ 1. Thus, the determination of the yield stress is intimately connected to the characterization of the wall slip of the viscoplastic suspension.

Rectangular slit flow:

The same apparent slip mechanism involving a particle-free "apparent slip" zone is assumed at the wall of the rectangular slit die which has a gap of 2B and a width of W with W>>2B. The velocity distributions for the three zones (I is the apparent slip layer, II is the deforming viscoplastic suspension and III is the plug flow region) are:

$$V_z^{\,I} = \left[\frac{-\partial P}{\partial z}\frac{B}{m_b}\right]^{s_b} \frac{B}{(s_b+1)}\left[1 - \left(\frac{y}{B}\right)^{s_b+1}\right] \quad \text{for } H \geq y \geq (H-\delta) \qquad (21)$$

with slip velocity $U_S = V_Z^{\,I}\Big|_{(B-\delta)}$

$$U_s = \frac{\tau_w^{\,s_b}}{m_b^{\,s_b}}\frac{B}{(s_b+1)}\left[1-\left(1-\frac{\delta}{B}\right)^{s_b+1}\right] \qquad (22)$$

Similar to the analysis followed for the capillary flow, the use of Binomial Theorem with $\left(1-\frac{d}{R}\right)^{s_b+1} \cong 1-\frac{\delta}{R}(s_b+1)$ provides $ß = \frac{d}{m_b{}^{s_b}}$ and $U_s = \frac{d}{m_b{}^{s_b}} t_w{}^{s_b}$. Thus, one obtains the same Navier´s slip coefficient, β, for the rectangular slit flow as determined for plane Couette flow and capillary flow.

Obtaining the same Navier´s slip coefficient, β, for both the drag flow based plane Couette flow and the pressure-driven capillary and rectangular slit flows is important. It justifies why wall slip data collected using steady torsional flow together with capillary rheometry should and do fall within the confines of a single wall slip velocity versus wall shear stress curve [Yilmazer and Kalyon (1989b); Kalyon et al. (1993)].

The velocity distribution for the deforming viscoplastic fluid in the rectangular slit is given as:

$$V_Z{}^{II} = U_s + \frac{B}{(s+1)}\frac{1}{\tau_w\ m^s}\left[\left(\tau_w\left(1-\frac{\delta}{B}\right)-\tau_0\right)^{s+1} - \left(\tau_w\ \frac{y}{B}-\tau_0\right)^{s+1}\right] \text{ for } y_0 \leq y \leq (h-\delta) \tag{23}$$

where $\tau_w = \frac{-\partial P}{\partial z}\frac{B}{2}$. The velocity of the plug, $V_Z{}^{III}$, for $0 \leq y \leq y_0$ (where y_0 is the location where the absolute value of the shear stress is equal to the yield stress) becomes:

$$V_Z{}^{III} = U_s + \frac{B}{(s+1)\tau_w\ m^s}\left(\tau_w\left(1-\frac{\delta}{B}\right)-\tau_0\right)^{s+1} \tag{24}$$

The volumetric flow rate Q (for $\delta \ll B$) is:

$$Q = Q_s + \frac{2WB^2}{(s+1)\tau_w{}^2}\frac{(\tau_w-\tau_0)^{s+1}}{m^s}\frac{[\tau_w(s+1)+\tau_0]}{(s+2)} \tag{25}$$

The derivative of the apparent shear rate, $(3Q/(2WB^2))$ versus the reciprocal half-gap, 1/B, at constant wall shear stress provides the wall slip velocity for rectangular slit flow:

$$\left.\frac{\partial\left(\frac{3Q}{2WB^2}\right)}{\partial(1/B)}\right|_{\tau_w} = 3U_s(\tau_w) \tag{26}$$

The true deformation rate of the suspension at the wall of the rectangular slit (for $\delta << B$)
can be determined from Equation (34) as:

$$\dot{\gamma}_w = \frac{(Q - Q_s)}{2WB^2}\left[2 + \frac{d\ln(Q - Q_s)}{d\ln\tau_w}\right] \tag{27}$$

Equation (27) can also be directly obtained from the integration of the velocity distribution using Leibniz rule of integration without assuming a constitutive behavior to the bulk fluid, similar to the capillary flow analysis [Kalyon (2003)].

Squeeze flow:

The analyses of the squeeze flow problem (where the suspension is sandwiched in between two discs one of which is stationary and the second is moving with a velocity normal to the plane of the disk) using various types of constitutive equations and wall boundary conditions are available (Scott 1931 and 1935; Covey and Stanmore 1981; Adams et al. 1994; Zhang et al. 1995; Laun et al. 1999; Lawal and Kalyon 1998 and 2000, Sherwood and Durban 1998; Meeten 2000). It is not possible to write analytical expressions for the squeeze flow of viscoplastic fluids which would also allow the wall slip velocity to be determined and more complicated analyses are necessary (Mannheimer 1983) and Tang and Kalyon (2004). Ahmed and Alexandrou (1994) modeled numerically the squeeze flow and used it to determine the parameters of the Herschel-Bulkley model. Tang and Kalyon (2004) have used a combination of squeeze and capillary flows to provide the data necessary for the solution of the inverse problem to characterize the three parameters of the Hershel-Bulkley equation and the two parameters of the wall slip velocity versus wall shear stress relationship.

Conclusions:

This paper outlines the basic mechanisms of wall slip and deformation occurring during the viscometric flows of energetic suspensions, which are generally fluids that exhibit a yield stress (viscoplastic) and apparent slip at the wall. The apparent slip layer is well defined and its thickness is a fraction of the particle diameter. For energetic suspensions the flow curves need to be collected as a function of the surface to volume ratio of the viscometer employed and the wall slip velocity values should be used to correct the shear rate at the wall. The corrections and the flow equations for various viscometers are provided and discussed.

Acknowledgements

I acknowledge with gratitude the help of my late colleague Dr. R. Yazici and Ms. E. Birinci for collecting the images given in Figures 3 and 4 and Dr. P. Yaras for the data given in Figure 9 and the input of Dr. H. Gevgilili.

References

Adams MJ, Edmondson B, Caughey DG, Yahya R (1994) An experimental and theoretical study of squeeze-film defomation and flow of elastoplastical fluids. J. Non-Newtonian Fluid Mech. 51:61-78

Ahmed A, Alexandrou AN (1994) Processing of semi-solid materials using a shearthickening Bingham fluid model," FED-vol. 179, Numerical Methods for Non-Newtonian Fluid Dynamics, ASME

Allende M. and D. Kalyon, "Assessment of Particle-Migration Effects in Pressure-Driven Viscometric Flows", J. Rheol. 44, 79-90 (2000).

Aral B. and D. M. Kalyon, "Effects of Temperature and Surface Roughness on Time-Dependent Development of Wall Slip in Torsional Flow of Concentrated Suspensions," J. Rheol. 38, 957-972 (1994).

Aral B. and D. M. Kalyon, "Viscoelastic Material Functions of Noncolloidal Suspensions with Spherical Particles," J. Rheol. 41, 599-620 (1997).

Barnes H., “A review of the slip (wall depletion) of polymer solutions, emulsions and particle suspensions in viscometers: its cause, character, and cure”, J. Non-Newtonian Fluid Mech., 56, 221-251 (1995).

Bingham, E. C., “Fluidity and Plasticity”, 231, McGraw Hill, London (1922).

Bird, B. B., R. Armstrong and O. Hassager, “Dynamics of Polymeric Liquids”, Volume 1, John Wiley and Sons, New York (1987).

Bird, B. B., W. Stewart and E. Lightfoot, “Transport Phenomena”, John Wiley and Sons, New York (2002).

Brunn, P., M. Muller and S. Bschorer, “Slip of complex fluids in viscometry”, Rheologica Acta, 35, 242-251 (1996).

Cohen, Y. and A. B. Metzner, “Apparent slip flow of polymer solutions“, J. Rheol. 29, 67-102 (1985).

Covey GH, Stanmore BR (1981) Use of the parallel-plate plastometer for the characterisation of viscous fluids with a yield stress. J. Non-Newtonian Fluid Mech 8:249-260

Denn, M. M. “Flow instabilities and wall slip”, Annu. Rev. Fluid Mech. 33, 265-287 (2001).

Fiske, T., S. Railkar and D. M. Kalyon, "Effects of Segregation on the Packing of Spherical and Non-Spherical Particles," Powder Technology, 81 57-64 (1994).

Gevgilili, H. and D.M. Kalyon, “Step Strain Flow: Wall Slip and other Error Sources”, J. Rheology, 45, 2, 467-475 (2001).

Gevgilili, H. “Development of the wall slip condition and its ramifications for polymers and other complex fluids”, PhD Thesis, Stevens Institute of Technology, Hoboken, NJ (2003).

Green, H., ”Further Development of the plastometer and its practical application to research and routine problems”, Proceedings Am. Soc. Testing Materials, II, 20, (1920).

Hatzikiriakos, S. and J. M. Dealy, “Wall slip of molten high density polyethylene. I. Sliding plate rheometer studies”, J. Rheol. 35, 497-523 (1991).

Jana, S., B. Kapoor and A. Acrivos, “Apparent wall slip velocity coefficients in concentrated suspensions of Noncolloidal particles”, J. Rheol. 39, 1123-1132 (1995).

Jiang, T., A. Young and A. B. Metzner, “The rheological characterization of HPG gels: Measurement of slip velocities in capillary tubes”, Rheol. Acta 25, 397-404 (1986).

Kalyon, D. M., Yazici, R., Jacob, C., Aral, B. and Sinton, S. W., 1991a, "Effects of Air Entrainment on the Rheology of Concentrated Suspensions during Continuous Processing," *Polym. Eng. Sci., 31*, 1386-1392 .

Kalyon, D. M., Jacob, C. and Yaras, P., 1991b, "An Experimental Study of the Degree of Fill and Melt Densification in Fully-intermeshing, Co-rotating Twin Screw Extruders," *Plastics, Rubber and Composites Processing and Applications, 16* (3), 193-200.

Kalyon, D., P. Yaras, B. Aral and U. Yilmazer, "Rheological Behavior of Concentrated Suspensions: A Solid Rocket Fuel Simulant," J. Rheol. 37, 35-53 (1993).

Kalyon, D., "Review of Factors Affecting the Continuous Processing and Manufacturability of Highly Filled Suspensions," Journal of Materials Processing and Manufacturing Science, 2 159-187 (1993).

Kalyon, D. and H. S. Gokturk, "Adjustable Gap Rheometer," U.S. Patent # 5,277,058 (1994).

Kalyon, D. "Highly Filled Materials: Understanding the Generic Behavior of Highly Filled Materials Leads to Manufacturing Gains and New Technologies," CHEMTECH, 25, 22-30 (1995).

Kalyon, D. M., H. Gokturk and I. Boz "An Adjustable Gap In-Line Rheometer," SPE ANTEC Technical Papers, 43, 2283-2288 (1997).

Kalyon, D., A. Lawal, R. Yazici, P. Yaras and S. Railkar, "Mathematical Modeling and Experimental Studies of Twin Screw Extrusion of Filled Polymers", Polym. Eng. Sci. 39, 1139-1151 (1999).

Kalyon, D., "Letter to the Editor: Comments on "A new method of processing capillary viscometry data in the presence of wall slip" [J. Rheol. 47, 337-348 (2003)]", J. Rheology, 47, 4, 187-1088 (2003).

Kalyon, D. and H. Gevgilili, "Wall slip and extrudate distortion of three polymer melts", J. Rheology, 47, 3, 683-699 (2003).

Laun HM, Rady M, Hassager O (1999) Analytical solutions for squeeze flow with partial wall slip, J. Non-Newtonian Fluid Mech., 81:1-15

Lawal A, Kalyon DM (1998) Squeeze flow of viscoplastic fluids subject to wall slip. Polymer Eng. Sci. 38:1793-1804

Lawal A, Kalyon DM (2000) Compressive squeeze flow of generalized Newtonian fluids with apparent wall slip. Intern. Polymer processing, XV:63-71

Leighton and Acrivos, "The shear-induced migration of particles in concentrated suspensions", J. Fluid Mech. 275, 155-199 (1987)

Mannheimer RJ (1983) Effect of slip on flow properties of cement slurries can flaw resistance calculations. Oil & Gas J 81:144-147

Meeten GH (2000) Yield stress of structured fluids measured by squeeze flow. Rheol. Acta 40:279-288

Metzner, A. B., “Rheology of suspensions in polymeric liquids”, J. Rheol. 29, 739-775 (1985).

Michienzi, M.A., C.M. Murphy, D. M. Kalyon and S. Railkar, Wall Slip and Capillary Flow Behavior of Extrudable Composite Propellant, Proceedings of JANNAF Conference Propellant Development and Characterization Subcommittee Meeting, Sunnyvale, California (1997).

Mooney M., “Explicit Formulas for slip and fluidity”, J. Rheol. 2, 210-222 (1931).

Ouchiyama, N. and T. Tanaka, “Porosity estimation for random packings of spherical particles”, Ind. Eng. Chem. Fund., 23, 490-493 (1984).

Prickett, S. E., C Murphy, W. Thomas and D. Kalyon, “Shear viscosity, extrudate swell and wall slip behavior of a double base propellant”, Proceedings of Joint Army, Navy, NASA, Air Force Propellant Development and Characterization Meeting, Charlottesville, VA, March 26 (2003).

Rabinowitsch, R., “Über the viskosität and elastizität von solen”, Z. Phys. Chem. Abt. A 145, 1-26 (1929).

Reiner, M., “Deformation, Strain and Flow”, H. K. Lewis and Co. Ltd., London (1960).

Russell, W. B. and M. Grant, “Distinguishing between dynamic yielding and wall slip in a weakly flocculated colloidal dispersion”, Colloids and Surfaces A. Physicochemical Eng. Aspects, 161, 271-282 (2000).

Scott JR (1931) Theory and application of the parallel-plate plastometer. Trans. Inst Rubber Ind 7:169-175

Sherwood JD, Durban D (1998) Squeeze-flow of a Herschel-Bulkley fluid. J. Non-Newtonian Fluid Mech 77:115-121

Soltani F. and U. Yilmazer, “Slip velocity and slip layer thickness in flow of concentrated suspensions”, J. Appl. Polym. Sci., 70, 515-522 (1998).

Suwardie, H., R. Yazici, D. M. Kalyon and S. Kovenklioglu, "Capillary Flow Behavior of Microcrystalline Wax and Silicon Carbide Suspension," J. Materials Sci. 33, 5059-5067 (1998).

Tang, H. and D. Kalyon, “Estimation of the parameters of Hershel-Bulkley fluid under wall slip using a combination of capillary and squeeze flow viscometers”, Rheol. Acta, 43, 80-88 (2004).

Walls, H., S. Caines, A. Sanchez and S. Khan, “Yield stress and wall slip phenomena in colloidal silica gels”, J. Rheol. 47, 847-868 (2003).

Yaras, P., D. M. Kalyon, and U. Yilmazer, "Flow Instabilities in Capillary Flow of Concentrated Suspensions," Rheologica Acta, 33, 48-59 (1994).

Yaras, P. “Rheological behavior and twin screw extrusion flow o non-colloidal concentrated suspensions”, PhD Thesis, Stevens Institute of Technology, Hoboken, NJ (1996).

Yeow, Y., H. Lee, A. Melvani and G. Mifsud, “A new method of processing capillary viscometry data in the presence of wall slip”, J. Rheol. 47, 337-348 (2003).

Yilmazer U., C. Gogos and D. M. Kalyon, "Mat Formation and Unstable Flows of Highly Filled Suspensions in Capillaries and Continuous Processors," Polymer Composites, 10, 242-248 (1989a).

Yilmazer U. and D. M. Kalyon, "Slip Effects in Capillary and Parallel Disk Torsional Flows of Highly Filled Suspensions," J. Rheol. 33, 1197-1212 (1989b).

Yilmazer U., and D. M. Kalyon, "Dilatancy of Concentrated Suspensions with Newtonian Matrices," Polymer Composites, 12, 226-232 (1991).

Yoshimura A. and R. K. Prud’homme, “Wall slip corrections for Couette and Parallel Disk Viscometers”, J. Rheol. 32, 53-67 (1988).

Zhang W, Silvi N, Vlachopoulos J (1995) Modeling and experiments of squeezing flow of polymer melts. Intern. Polymer processing X:155-164

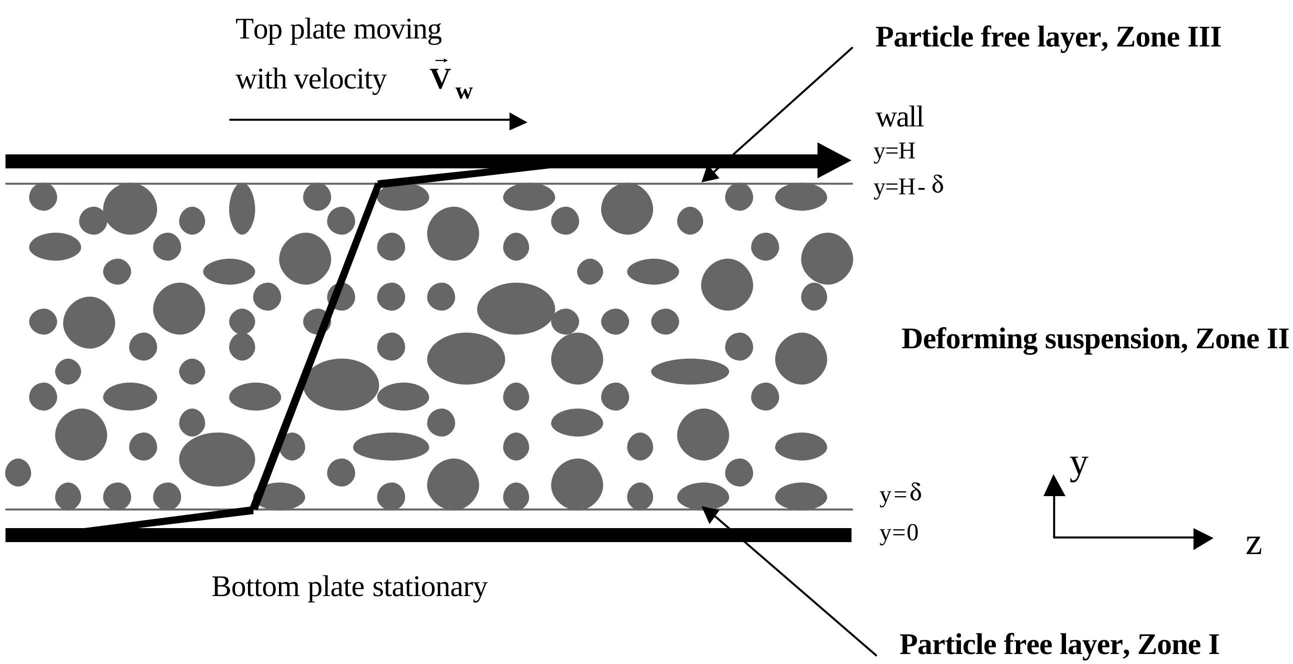
Top plate moving
with velocity $\vec{V}_w$
Particle free layer, Zone III
wall
y=H
y=H- δ
Deforming suspension, Zone II
y
y=δ
y=0
z
Bottom plate stationary
Particle free layer, Zone I

Figure 1

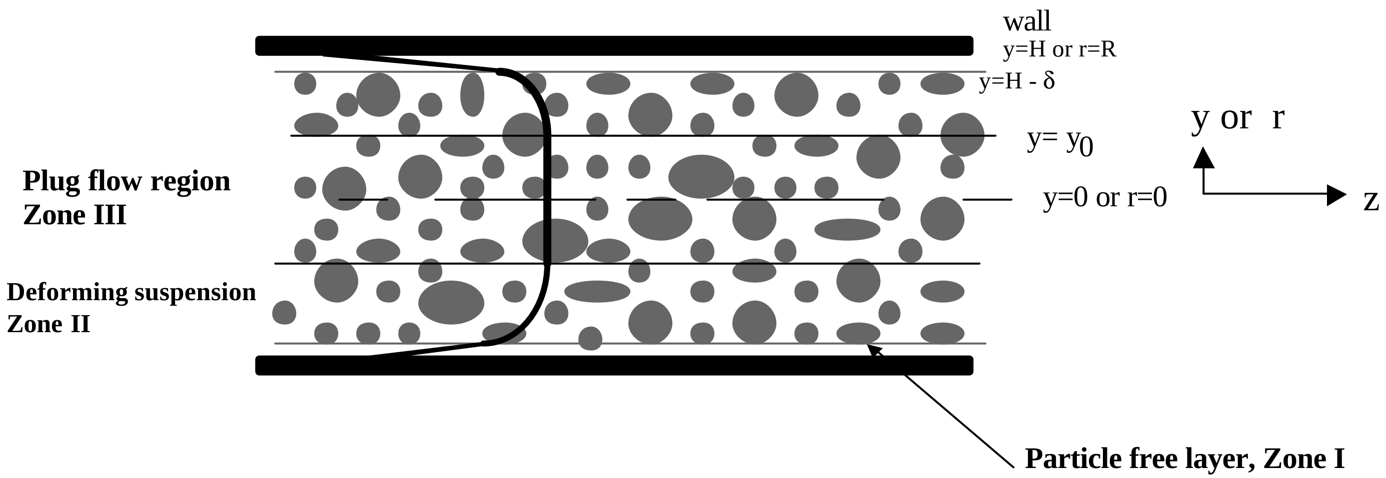
wall
y=H or r=R
y=H - δ
y= y0
y=0 or r=0
y or r
z
Plug flow region
Zone III
Deforming suspension
Zone II
Particle free layer, Zone I

Figure 2

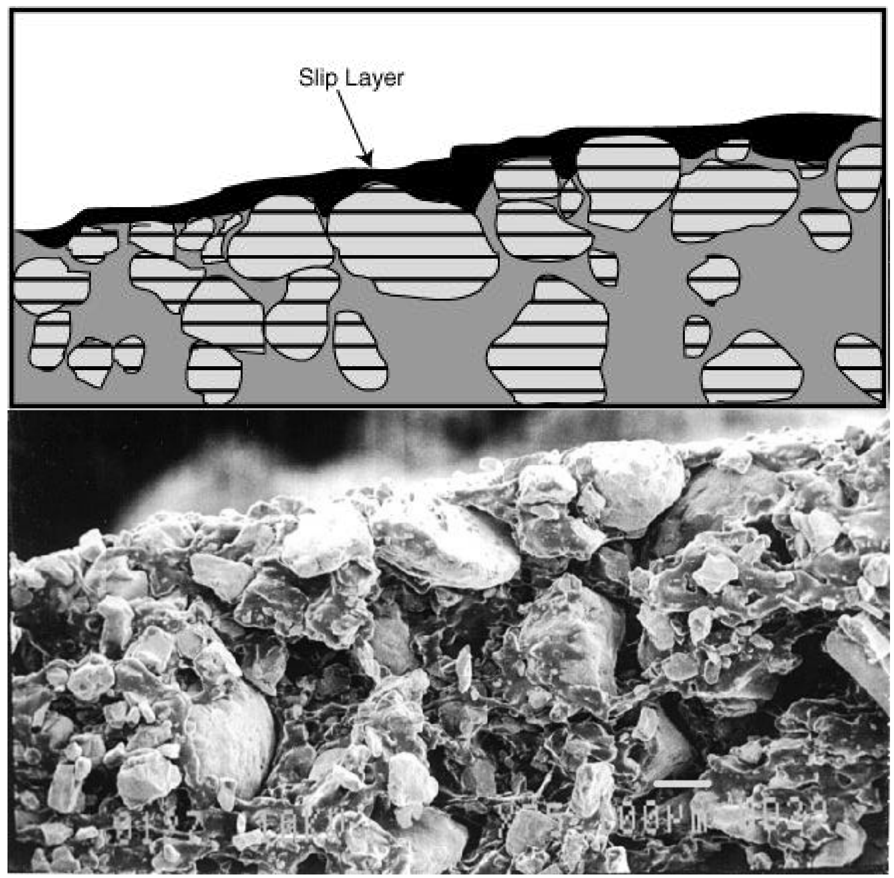

Figure 3

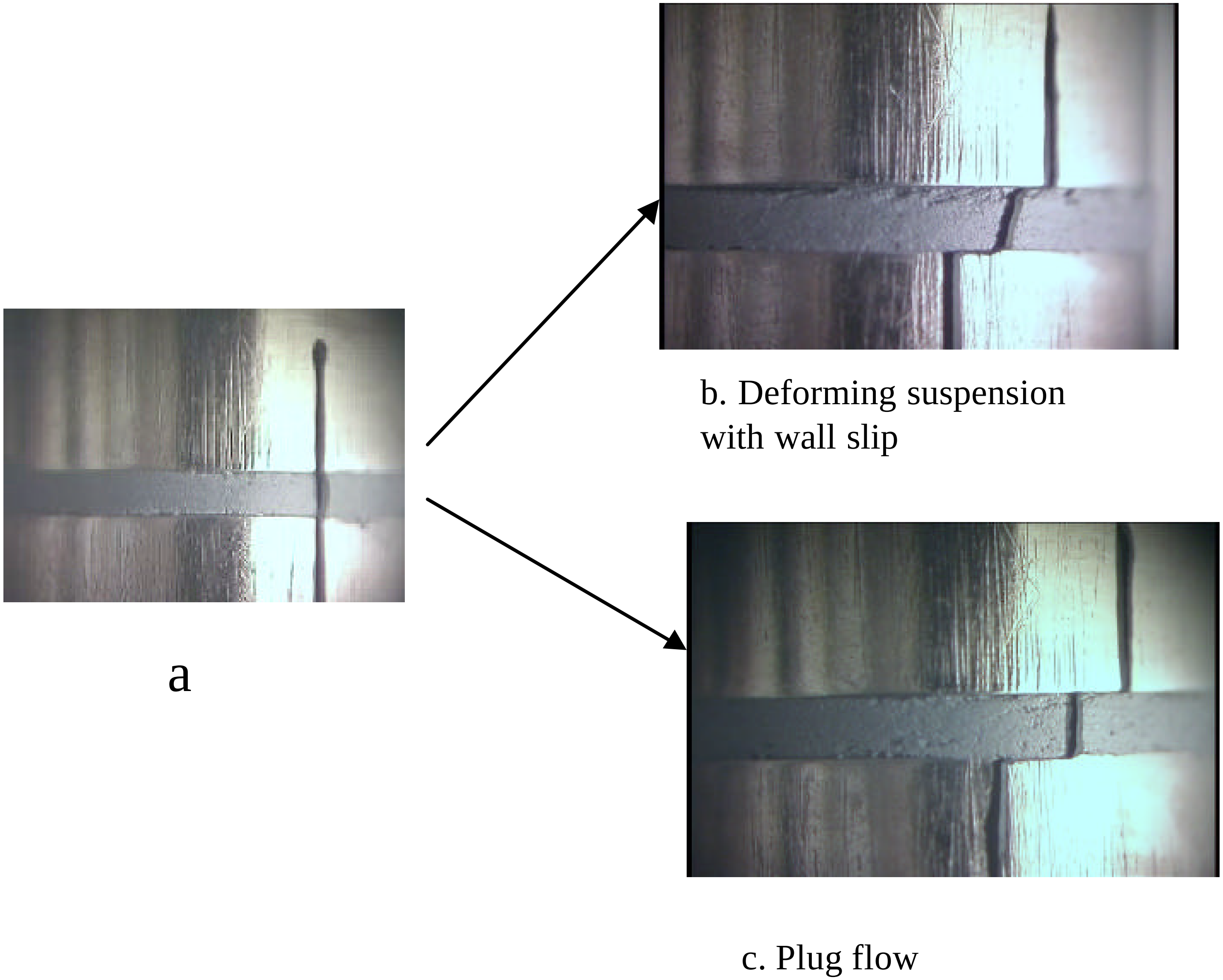

Figure 4

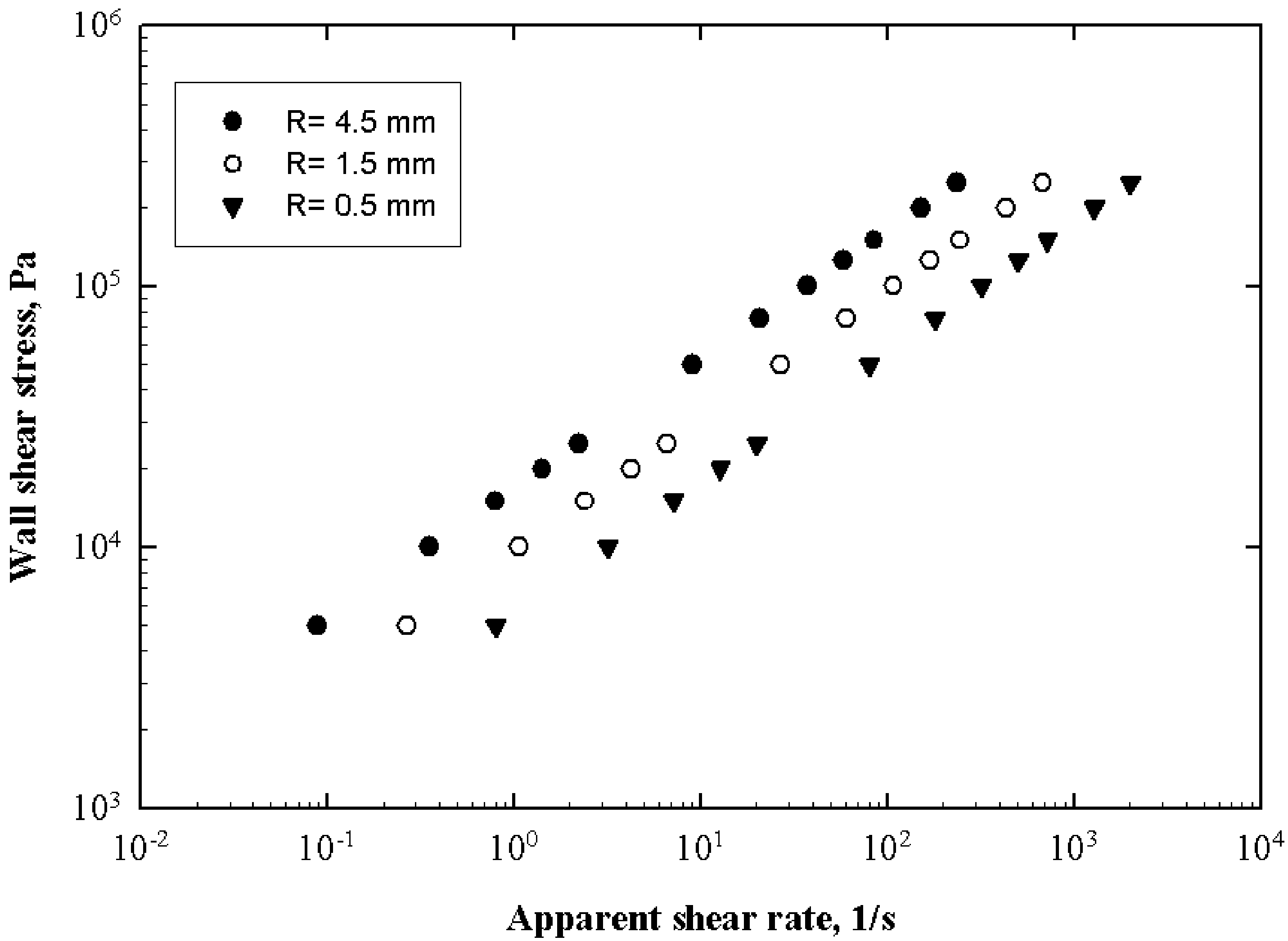

R= 4.5 mm
R= 1.5 mm
R= 0.5 mm
Wall shear stress, Pa
Apparent shear rate, 1/s
10^{3}
10^{4}
10^{5}
10^{6}
10^{-2}
10^{-1}
10^{0}
10^{1}
10^{2}
10^{3}
10^{4}

Figure 5

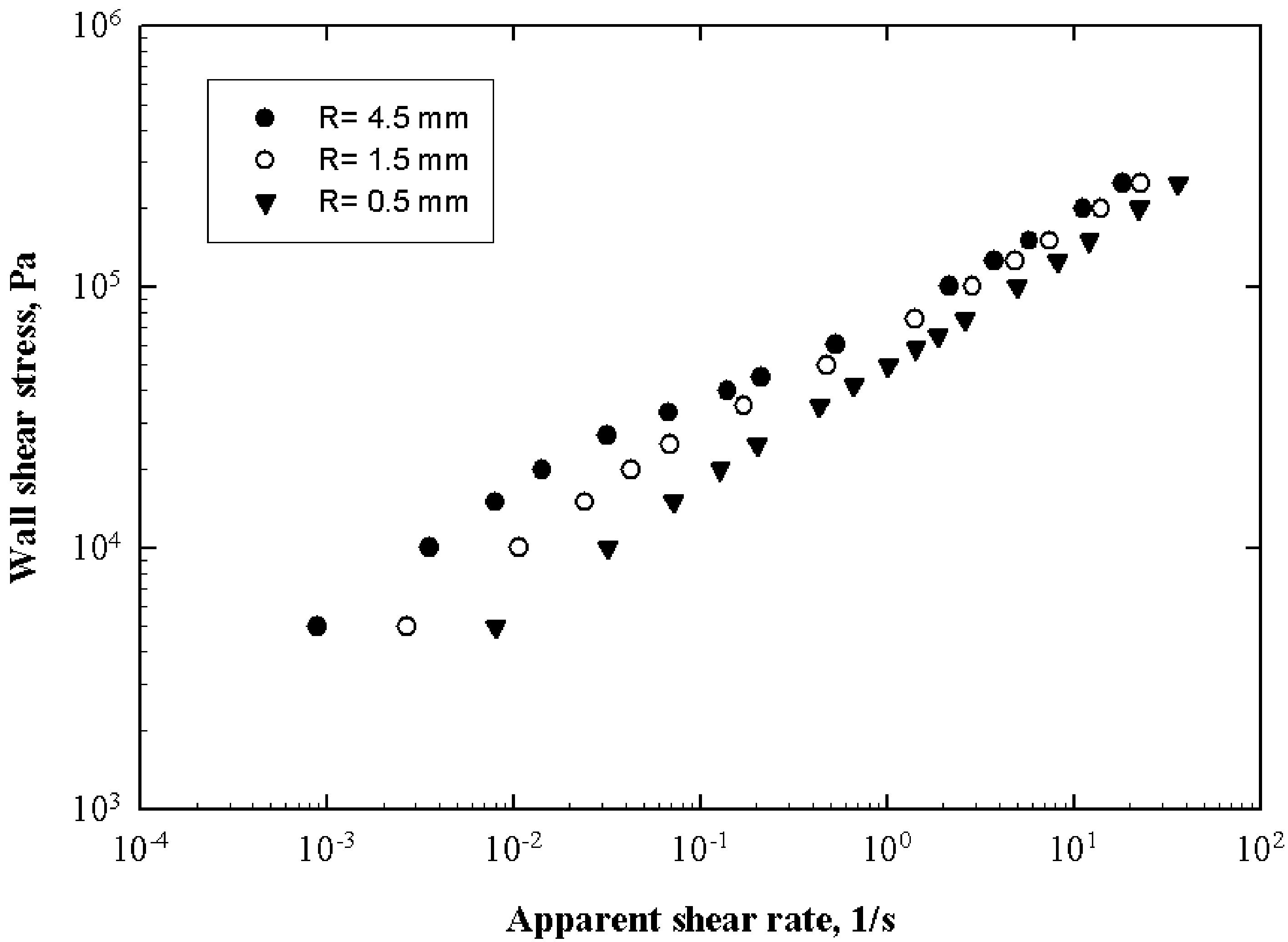

R= 4.5 mm
R= 1.5 mm
R= 0.5 mm
Wall shear stress, Pa
Apparent shear rate, 1/s
10^{6}
10^{5}
10^{4}
10^{3}
10^{-4}
10^{-3}
10^{-2}
10^{-1}
10^{0}
10^{1}
10^{2}

Figure 6

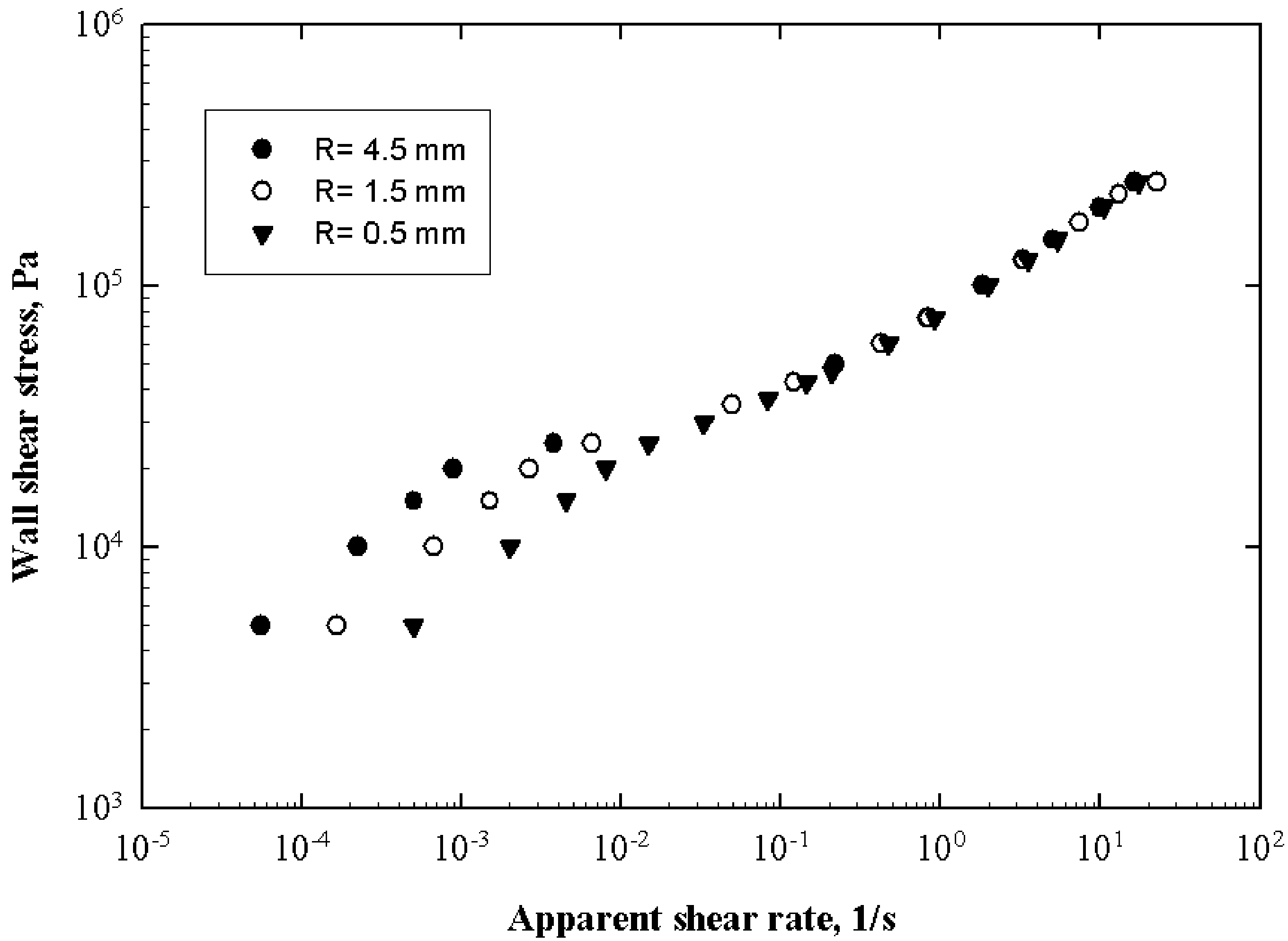

R= 4.5 mm
R= 1.5 mm
R= 0.5 mm
Wall shear stress, Pa
Apparent shear rate, 1/s
10^{6}
10^{5}
10^{4}
10^{3}
10^{-5}
10^{-4}
10^{-3}
10^{-2}
10^{-1}
10^{0}
10^{1}
10^{2}

Figure 7

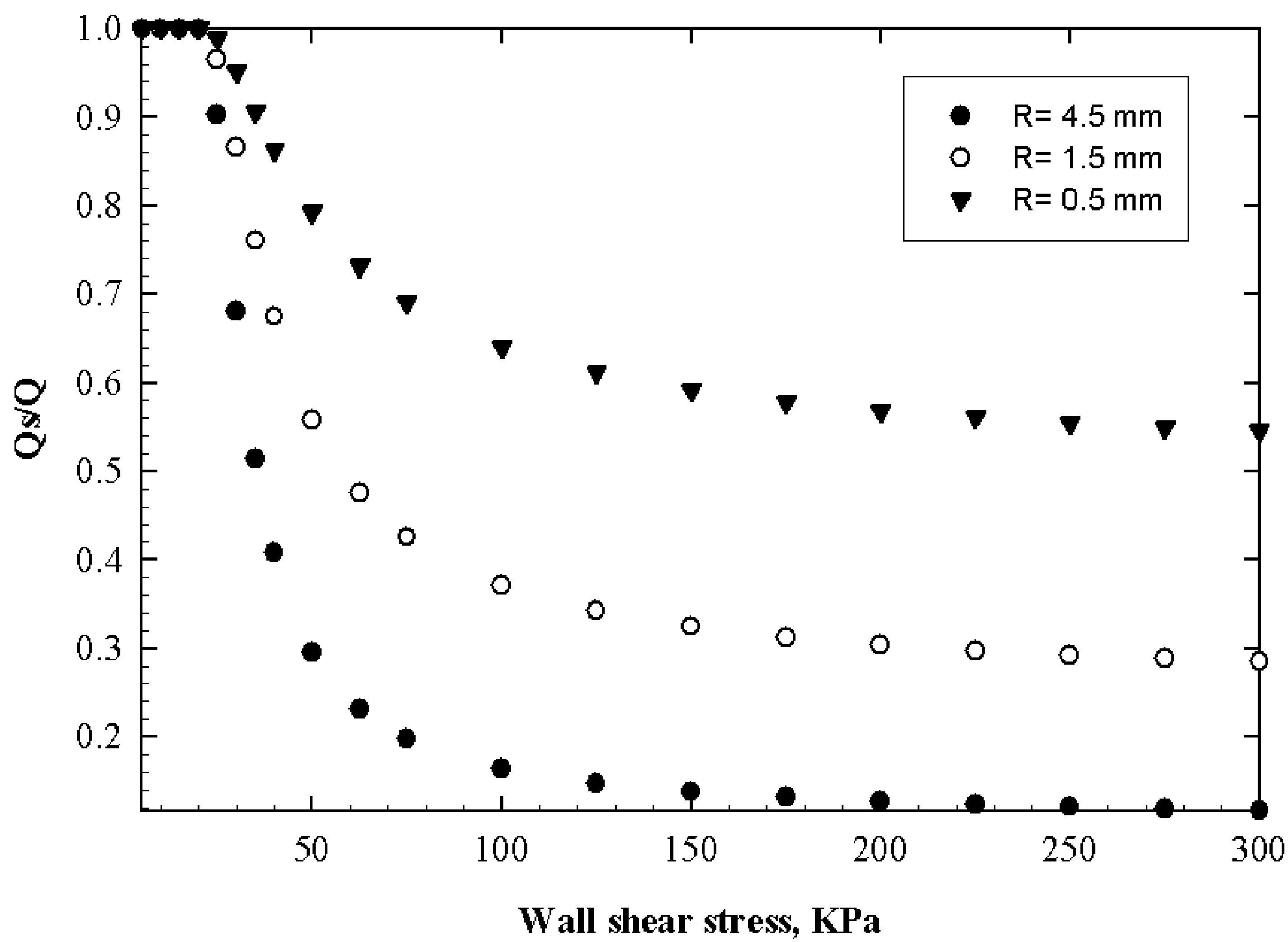
R= 4.5 mm
R= 1.5 mm
R= 0.5 mm
Qs/Q
1.0
0.9
0.8
0.7
0.6
0.5
0.4
0.3
0.2
50
100
150
200
250
300
Wall shear stress, KPa

Figure 8

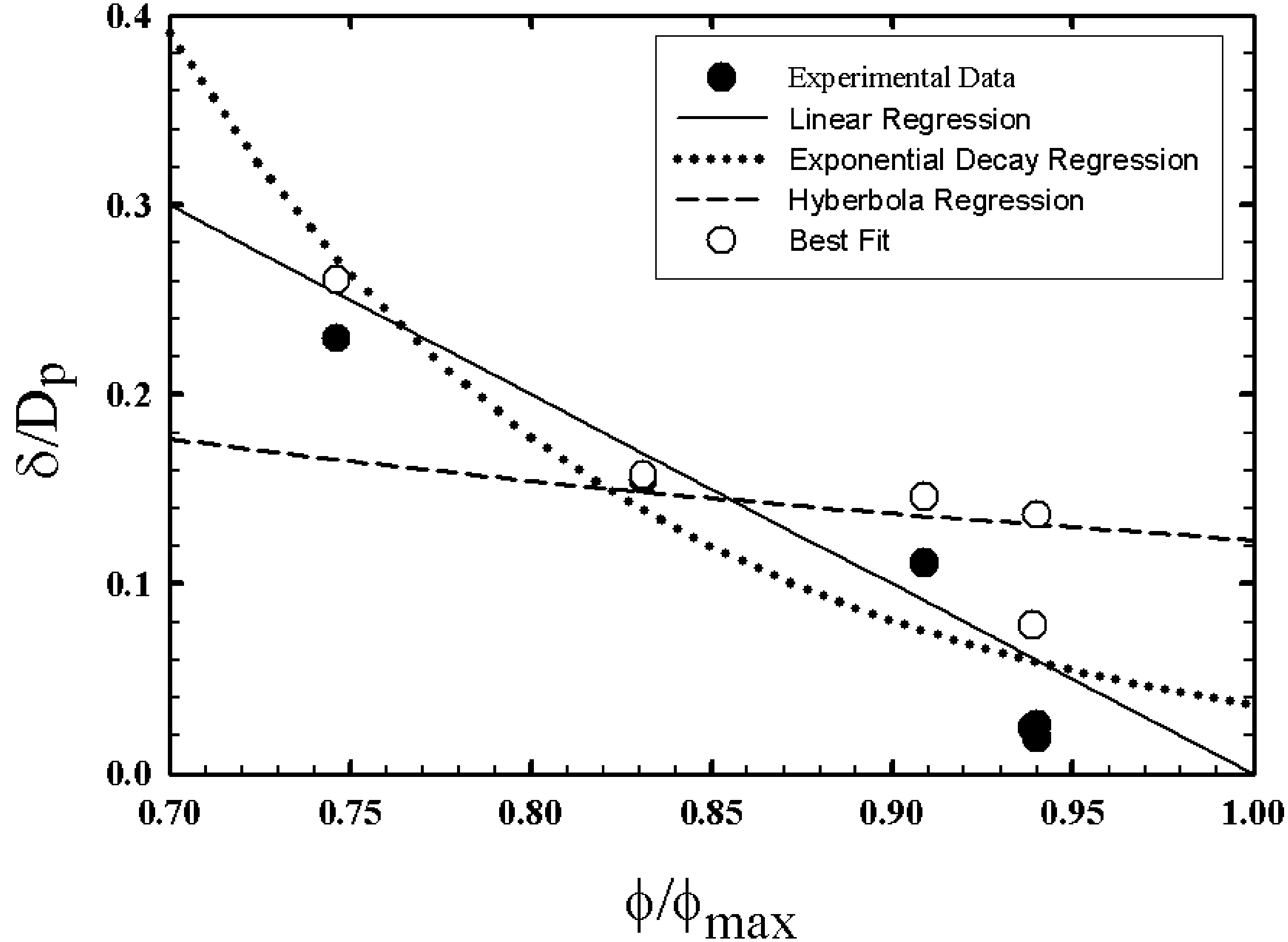

Linear

$$\frac{\delta}{D_p} = 1 - \frac{\phi}{\phi_m}$$

Exponential

$$\frac{\delta}{D_p} = \left(100 \times e^{-8*\frac{\phi}{\phi_m}}\right)$$

Hyperbolic

$$\frac{\delta}{D_p} = \frac{100}{1 + \frac{1}{.0012}\frac{\phi}{\phi_m}}$$

Figure 9